

2004

# Stimulated emission and time-resolved photoluminescence in rf-sputtered ZnO thin films

Ü. Özgür

*Virginia Commonwealth University, uozgur@vcu.edu*

A. Teke

*Virginia Commonwealth University*

C. Liu

*Virginia Commonwealth University*

*See next page for additional authors*

Follow this and additional works at: [http://scholarscompass.vcu.edu/egre\\_pubs](http://scholarscompass.vcu.edu/egre_pubs)

 Part of the [Electrical and Computer Engineering Commons](#)

Özgür, Ü., Teke, A., Liu, C., et al. Stimulated emission and time-resolved photoluminescence in rf-sputtered ZnO thin films. *Applied Physics Letters*, 84, 3223 (2004). Copyright © 2004 AIP Publishing LLC.

---

Downloaded from

[http://scholarscompass.vcu.edu/egre\\_pubs/134](http://scholarscompass.vcu.edu/egre_pubs/134)

This Article is brought to you for free and open access by the Dept. of Electrical and Computer Engineering at VCU Scholars Compass. It has been accepted for inclusion in Electrical and Computer Engineering Publications by an authorized administrator of VCU Scholars Compass. For more information, please contact [libcompass@vcu.edu](mailto:libcompass@vcu.edu).

---

**Authors**

Ü. Özgür, A. Teke, C. Liu, S.-J. Cho, Hadis Morkoç, and H. O. Everitt

## Stimulated emission and time-resolved photoluminescence in rf-sputtered ZnO thin films

Ü. Özgür,<sup>a)</sup> A. Teke,<sup>b)</sup> C. Liu, S.-J. Cho, and H. Morkoç

*Department of Electrical Engineering, Virginia Commonwealth University, Richmond, Virginia 23284*

H. O. Everitt<sup>c)</sup>

*Department of Physics, Duke University, Durham, North Carolina 27708*

(Received 7 January 2004; accepted 25 February 2004)

Stimulated emission (SE) was measured from ZnO thin films grown on *c*-plane sapphire by rf sputtering. Free exciton transitions were clearly observed at 10 K in the photoluminescence (PL), transmission, and reflection spectra of the sample annealed at 950 °C. SE resulting from both exciton-exciton scattering and electron hole plasma formation was observed in the annealed samples at moderate excitation energy densities. The SE threshold energy density decreased with increasing annealing temperature up to ~950 °C. The observation of low threshold exciton-exciton scattering-induced SE showed that excitonic laser action could be obtained in rf-sputtered ZnO thin films. At excitation densities below the SE threshold, time-resolved PL revealed very fast recombination times of ~74 ps at room temperature, and no significant change at 85 K. The decay time for the SE-induced PL was below the system resolution of <45 ps. © 2004 American Institute of Physics. [DOI: 10.1063/1.1713034]

ZnO received much attention as a promising material for optoelectronic devices such as UV laser diodes and UV-blue light-emitting diodes owing to its high exciton binding energy of 60 meV.<sup>1,2</sup> The most recent reports on *p*-type doping<sup>3</sup> and the availability of high quality bulk ZnO<sup>2,4-6</sup> for homoepitaxial growth of thin films have provided unprecedented capabilities for device applications. Stimulated emission (SE) and lasing, which could survive even at temperatures as high as 550 K, have been observed in ZnO thin films.<sup>7</sup> Among various thin film deposition techniques, including molecular beam epitaxy (MBE) and metalorganic chemical vapor deposition (MOCVD), which are reported to produce very high quality material, rf magnetron sputtering of ZnO thin films has the advantages of process simplicity and low temperature deposition, and the deposited films have good orientation with close to single-crystal morphology. Additionally, both *n*- and *p*-type doping in ZnO films have been achieved by rf magnetron sputtering.<sup>3,8</sup> In this letter, optical properties of rf-sputtered ZnO epilayers subjected to postgrowth thermal treatment are explored by measuring their SE and time-resolved photoluminescence (TRPL) characteristics. We report the observation of exciton-exciton scattering related SE in ZnO thin films grown by the simple sputtering technique. The effect of SE accelerated carrier decay on TRPL is also investigated.

A ~350 nm-thick ZnO layer was deposited directly on *c*-plane sapphire at 650 °C by rf-magnetron sputtering in an Ar+O<sub>2</sub> ambient atmosphere. To achieve better crystal structure, postdeposition annealing was performed at 800, 950, and 1000 °C on different pieces cut from the same sample.

Annealing increases atomic mobility, increasing the ability of atoms to find the most energetically favored sites, thereby achieving better crystal structure and a more relaxed ZnO film. Another sample with a thickness of ~100 nm was also grown under the same conditions and annealed at 950 °C. This thinner sample was only used in transmission experiments for identification of the excitonic transitions.

Both x-ray diffraction (XRD) rocking curve and atomic force microscopy (AFM) measurements were carried out for structural and morphological characterization. The results are summarized in Table I. The samples annealed at 950 and 1000 °C showed the sharpest (0002) peak and the smallest rms surface roughness. The (0002) rocking curve peaks were Gaussian and showed no tail caused by the deformed interfacial regions.<sup>9</sup> For the 950 °C sample, AFM revealed a grain size distribution between 80 and 200 nm. The grain size decreased with decreasing annealing temperature. The microcrystallite grain formation and its effects on optical gain in ZnO have been previously discussed for ZnO samples grown by MBE.<sup>10,11</sup>

Continuous-wave (cw) photoluminescence (PL) and transmission/reflection measurements were performed at 10 K using a 25 mW HeCd laser operating at 325 nm (3.82 eV) and a 20 W tungsten lamp, respectively. A photomultiplier tube attached to a 1.25 m grating spectrometer was used for

TABLE I. Structural and optical parameters for the ZnO samples obtained from AFM, XRD, and PL measurements.

Annealing temperature	rms surface roughness (nm)	XRD (0002)	
		FWHM (arcmin)	10 K PL FWHM (meV)
As-grown	14.8	66.0	10
800 °C	13.5	25.1	3.8
950 °C	7.5	16.9	2.7
1000 °C	6.8	16.2	3.0

<sup>a)</sup>Electronic mail: uozgur@vcu.edu

<sup>b)</sup>Also at Balikesir University, Faculty of Arts and Science, Department of Physics, 10100, Balikesir, Turkey

<sup>c)</sup>Also at the U.S. Army Research Office, Research Triangle Park, Durham, North Carolina 27709

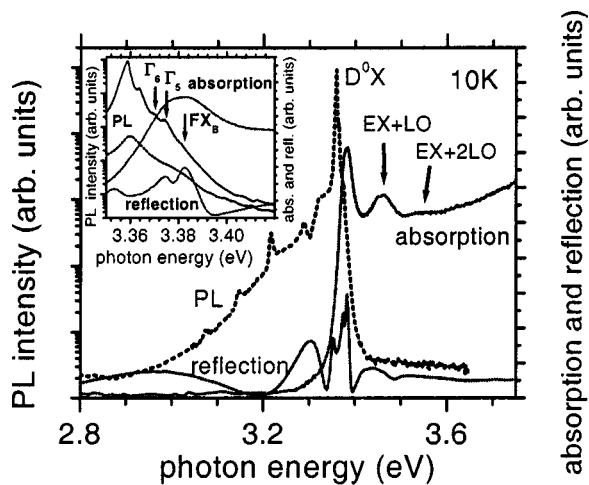


FIG. 1. 10 K PL ( $E \perp c$ ) and reflection (unpolarized light) data for the 350 nm-thick, and absorption (unpolarized light) data for the 100 nm-thick ZnO samples annealed at 950 °C. The inset shows an enlarged version of the free excitonic region of the spectrum. The PL for the as-grown sample (dotted line) is also shown (inset) for comparison.

detection. The 950 °C sample showed the highest quantum efficiency and the narrowest PL linewidth (Table I). The low temperature PL is dominated by the donor bound exciton transition ( $D^0X$ : 3.359 eV at 10 K) up to 120 K, while the room temperature emission was purely free excitonic and occurred at 3.294 eV. As shown in Fig. 1 for excitation polarization perpendicular to the  $c$  axis ( $E \perp c$ ), the free exciton emission lines<sup>4</sup> ( $FX_A$ - $\Gamma_6$ : 3.370 eV,  $FX_A$ - $\Gamma_5$ : 3.374 eV,  $FX_B$ : 3.381 eV) were clearly visible for the 950 °C sample. Analyzing the temperature dependence of the free exciton emission intensity,<sup>12</sup> the binding energy is obtained as  $\sim 60$  meV.

Further analysis of the free exciton transitions was carried out for the 950 °C sample by transmission and reflection measurements with unpolarized light. Although the free exciton transitions,  $A$  (3.376 eV) and  $B$  excitons (3.388 eV) are easily identified in the reflection spectrum in Fig. 1, the absorption for the 100 nm-thick 950 °C sample shows the  $A$  and  $B$  excitons only as shoulders of the wide excitonic peak due to the line broadening caused by interface roughness. The observation of particularly strong free excitonic features further emphasizes the fact that high quality ZnO thin films can be grown by rf sputtering. The additional features at 3.46 and 3.55 eV are attributed to exciton-LO phonon complex transitions.<sup>13,14</sup> The lattice mismatch-induced inhomogeneous strain distribution results in a Stokes shift of  $< 10$  meV.

Pulsed excitation, time-integrated PL (TI-PL) was performed on the samples at room temperature using  $\sim 100$  fs-wide pulses from a 1 kHz optical parametric amplifier. The 3.82 eV pulsed excitation was incident 45° to the surface normal, and the TI-PL, which was collected normal to the surface, was detected by a charge-coupled device camera attached to a 30 cm grating spectrometer. The spectrally-integrated PL intensities were plotted as a function of pump energy density to obtain the SE thresholds ( $I_{th}$ ). The spontaneous emission (SPE) peak for 5  $\mu\text{J}/\text{cm}^2$  excitation occurred at 3.285 eV, compared to 3.294 eV under cw excita-

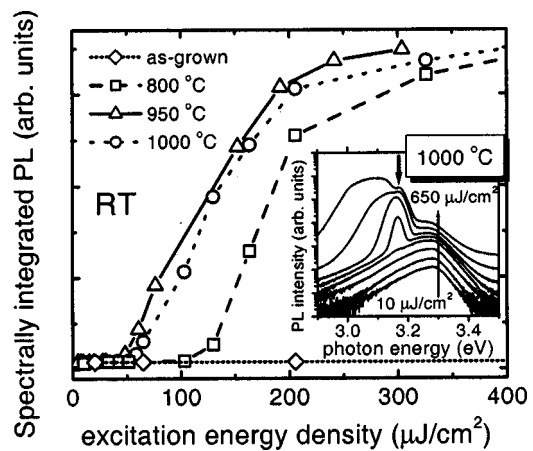


FIG. 2. Room temperature (RT) spectrally integrated PL for the ZnO samples normalized to the spontaneous emission. The inset shows the spectrally-resolved PL for the 1000 °C sample for different excitation densities. The downward-pointing arrow in the inset indicates the exciton-exciton scattering-induced SE peak.

tion, and continued to redshift with increasing excitation density due to bandgap renormalization.

SE features are observed for all the annealed samples; however, the as-grown sample did not show any sign of SE for the maximum energy density used here. The spectrally-resolved TI-PL for the 1000 °C sample is shown in Fig. 2 inset. For excitation densities above  $\sim 50 \mu\text{J}/\text{cm}^2$  SE emerges at 3.167 eV as a sharp feature on the lower energy side of the SPE peak and grows superlinearly. This SE peak has been attributed to exciton-exciton scattering and lies below the free exciton energy by an exciton binding energy plus the mean kinetic energy  $3/2 k_B T$ ,<sup>7,15</sup> where  $k_B T$  is the thermal energy. This peak then slightly redshifts to 3.160 eV since the inelastic exciton-exciton scattering leaves one exciton in an excited state which in turn reduces the emission energy of the recombining exciton.<sup>15</sup> As the excitation density is increased above 250  $\mu\text{J}/\text{cm}^2$ , a second peak emerges at 3.133 eV due to SE from the electron hole plasma (EHP). At these higher excitation densities, phase space filling and Coulomb interactions cause excitons to lose their individual character by ionization and eventually an EHP is formed. This EHP-induced SE peak shifts and broadens with increasing excitation as a result of bandgap renormalization. The coexistence of the exciton-exciton scattering and the EHP originates from the spatial nonuniformity of the sample as well as the laser beam profile, i.e., the EHP and the exciton-exciton scattering induced SE may come from different regions of the sample excited by the laser.

The SE peak attributed to exciton-exciton scattering is also observed for the 950 °C sample, but not for the 800 °C sample. Due to the existence of exciton-exciton scattering,  $I_{th}$  for the 950 and 1000 °C samples (49 and 58  $\mu\text{J}/\text{cm}^2$ , respectively) were significantly lower than that for the 800 °C sample (130  $\mu\text{J}/\text{cm}^2$ ). Figure 2 shows the PL data spectrally integrated between 3.1 and 3.4 eV for all the samples. It has been suggested that the exciton-exciton peak only appears in high quality ZnO samples grown mostly by MBE and MOCVD techniques.<sup>7,16</sup> Here, it is shown that the ZnO layers grown by the simpler rf sputtering technique may

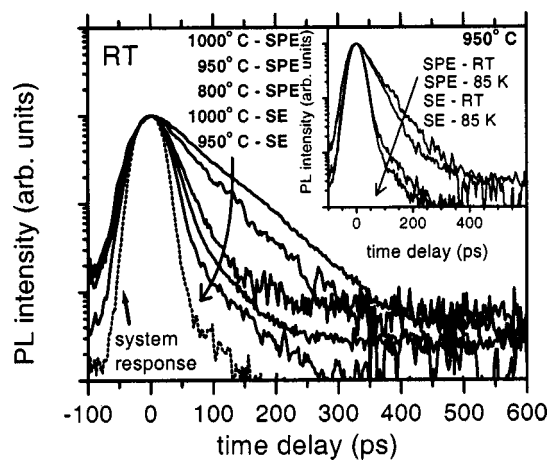


FIG. 3. RT TRPL for the SPE and the SE from the annealed ZnO samples. The inset shows the 85 K and RT TRPL data for the sample annealed at 950 °C.

have similar optical quality sufficient for excitonic laser action.

In order to investigate the effects of annealing and SE on carrier dynamics, TRPL spectroscopy was employed at room temperature and at 85 K using a  $\sim 45$  ps-resolution Hamamatsu streak camera. Figure 3 shows the TRPL data for all the annealed samples at room temperature. The excitation densities were kept slightly below  $I_{th}$  ( $\sim 30 \mu\text{J}/\text{cm}^2$ ) to measure the SPE decay times, while high excitation densities ( $\sim 200 \mu\text{J}/\text{cm}^2$ ) were used to observe the recombination dynamics under the influence of SE. Single exponential decay fits revealed the spontaneous recombination times as 74, 59, and 30 ps for the 1000, 950, and 800 °C samples, respectively. The decay time for the as-deposited sample (not shown) was below the system resolution. Here, it should be noted that no deconvolution of the system response was performed on the TRPL data. The increase of the decay times with annealing temperature suggests reduction of nonradiative recombination centers. As expected, SE-induced recombination occurs very fast ( $< 30$  ps). TRPL data for above  $I_{th}$  excitations also show a much weaker and slower decaying component visible after the SE is over ( $\sim 55$  ps) with the characteristic decay time of the spontaneous recombination.

The spontaneous recombination times observed here for the rf-sputtered ZnO thin films are comparable with the values in the literature. Guo *et al.*<sup>17</sup> reported 30 ps room temperature excitonic recombination times for ZnO thin films grown on Si by MOCVD. Koida *et al.*<sup>18</sup> measured recombination times of up to 110 ps for good quality ZnO thin films grown on  $\text{ScAlMgO}_4$  substrates by MBE. These decay times, including the ones measured here, are much shorter than those reported for single crystal ZnO<sup>4,17</sup> most probably due to effective nonradiative recombination in thin films at room temperature. Surprisingly, TRPL measurements performed at 85 K did not show any significant change in decay times. The inset in Fig. 3 compares the room temperature and the 85 K TRPL data of the 950 °C sample for both below and above  $I_{th}$  (950 °C). At 85 K the SPE decay time is 49 ps indicating that an effective nonradiative recombination

mechanism is still present. However, the characteristic single exponential decay along with the strong photon emission suggests that the radiative decay component is also fast. The slight decrease in the decay time at 85 K may be explained by increased absorption at low temperatures and the weak carrier density dependence of the recombination times.

In summary, low  $I_{th}$  due to exciton-exciton scattering were observed in rf-sputtered ZnO thin films subjected to postgrowth annealing. For higher excitation densities SE from an EHP was also observed. SE-induced carrier decay was measured to occur faster than 30 ps. TRPL measurements for below  $I_{th}$  excitation revealed spontaneous recombination times as long as 74 ps at room temperature for the 1000 °C sample. Even though these fast recombination times indicate effective nonradiative centers, the absence of a secondary exponential decay and high emission intensities suggest that radiative recombination should also occur very fast. This is also supported by the fact that measurements at 85 K produce similar timescales.

This work was supported by the AFOSR (Dr. T. Steiner) and the ONR (Dr. C. E. C. Wood), and benefitted from the SBIR grant by MBO through Cermet Inc. and monitored by Dr. C. Litton. The VCU team also benefitted from a long-time collaboration with Cermet, Inc., which produces high quality ZnO substrates. The Duke portion of this work was funded in part by U.S. Army Research Office Grant No. DAAG55-98-D-0002.

- <sup>1</sup>D. C. Look, *Mater. Sci. Eng., B* **80**, 383 (2001).
- <sup>2</sup>D. C. Reynolds, D. C. Look, B. Jogai, C. W. Litton, G. Cantwell, and W. C. Harsch, *Phys. Rev. B* **60**, 2340 (1999).
- <sup>3</sup>K.-K. Kim, H.-S. Kim, D.-K. Hwang, J.-H. Lim, and S.-J. Park, *Appl. Phys. Lett.* **83**, 63 (2003).
- <sup>4</sup>A. Teke, Ü. Özgür, S. Doğan, X. Gu, H. Morkoç, B. Nemeth, J. Nause, and H. O. Everitt (unpublished).
- <sup>5</sup>M. Suscavage, M. Harris, D. Bliss, P. Yip, S.-Q. Wang, D. Schwall, L. Bouthillette, J. Bailey, M. Callahan, D. C. Look, D. C. Reynolds, R. L. Jones, and C. W. Litton, *MRS Internet J. Nitride Semicond. Res.* **4S1**, G3.40 (1999).
- <sup>6</sup>E. Ohshima, H. Ogino, I. Niikura, K. Maeda, M. Sato, M. Ito, and T. Fukuda, *J. Cryst. Growth* **260**, 166 (2004).
- <sup>7</sup>D. M. Bagnall, Y. F. Chen, Z. Zhu, T. Yao, M. Y. Shen, and T. Goto, *Appl. Phys. Lett.* **73**, 1038 (1998).
- <sup>8</sup>K.-K. Kim, J.-H. Song, H.-J. Jung, W.-K. Choi, S.-J. Park, J.-H. Song, and J.-Y. Lee, *J. Vac. Sci. Technol. A* **18**, 2864 (2000).
- <sup>9</sup>Y. Chen, D. Bagnall, and T. Yao, *Mater. Sci. Eng., B* **75**, 190 (2000).
- <sup>10</sup>M. Kawasaki, A. Ohtomo, I. Ohkubo, H. Koinuma, Z. K. Tang, P. Yu, G. K. L. Wong, B. P. Zhang, and Y. Segawa, *Mater. Sci. Eng., B* **56**, 239 (1998).
- <sup>11</sup>P. Zu, Z. K. Tang, G. K. L. Wong, M. Kawasaki, A. Ohtomo, H. Koinuma, and Y. Segawa, *Solid State Commun.* **103**, 459 (1997).
- <sup>12</sup>D. W. Hamby, D. A. Lucca, M. J. Klopffstein, and G. Cantwell, *J. Appl. Phys.* **93**, 3214 (2003).
- <sup>13</sup>W. Y. Liang and A. D. Yoffe, *Phys. Rev. Lett.* **20**, 59 (1968).
- <sup>14</sup>T. Makino, C. H. Chia, N. T. Tuan, H. D. Sun, Y. Segawa, M. Kawasaki, A. Ohtomo, K. Tamura, and H. Koinuma, *Appl. Phys. Lett.* **77**, 975 (2000).
- <sup>15</sup>Y. Chen, N. T. Tuan, Y. Segawa, H.-J. Ko, S.-K. Hong, and T. Yao, *Appl. Phys. Lett.* **78**, 1469 (2001).
- <sup>16</sup>A. Ohtomo, M. Kawasaki, Y. Sakurai, Y. Yoshida, H. Koinuma, P. Yu, Z. K. Tang, G. K. L. Wong, and Y. Segawa, *Mater. Sci. Eng., B* **54**, 24 (1998).
- <sup>17</sup>B. Guo, Z. R. Qiu, and K. S. Wong, *Appl. Phys. Lett.* **82**, 2290 (2003).
- <sup>18</sup>T. Koida, S. F. Chichibu, A. Uedono, A. Tsukazaki, M. Kawasaki, T. Sota, Y. Segawa, and H. Koinuma, *Appl. Phys. Lett.* **82**, 532 (2003).